Concept design of a sounding rocket main structure using high performance materials

Pedro Miguel Gomes Silva
pedromiguelsilva98@tecnico.ulisboa.pt

Instituto Superior Técnico, Universidade de Lisboa, Portugal

December 2021

Abstract

In recent years, there has been a growing interest and investment in new space technologies. This interest has different magnitudes, from the goals of getting the first human to Mars, and returning to the Moon, but also a new era of space tourism. In addition, there has been an increasing investment in launching new satellites, but also in launching rockets to carry out all kinds of measuring instruments to space, also named sounding rocket. This is where the interest of CEiiA arises leading to this work addressing the initial development of this rocket. This work was developed in collaboration with CEiiA and aims to develop the design of a sounding rocket, as well as the study of some of its components. Based on the mission objectives and requirements, and in conjunction with examples from other launchers, the sounding rocket design was established. Then, some of the components of the sounding rocket were studied with a finite element analysis using the *NX Siemens* software to perform the simulations based on the applied loads. This study was carried out using different materials such as aluminium and carbon fiber-reinforced polymer (CFRP). In general, composites present an advantageous solution by allowing a reduction in weight while maintaining the structural integrity of the rocket. However, composite materials also have some disadvantages, namely possible compatibility problems with liquid oxygen, thus making aluminum an alternative solution. The work developed was essentially focused on preliminary rocket design and a more detailed work is essential for the future.
Keywords: sounding rocket, CFRP composites and sandwich, aluminium, finite elements analysis

1. Introduction

Nowadays, space is available to different players from governments to private companies. Different types of rockets are needed to accomplish the goals of each mission, from rockets taking humans to space, to rockets carrying large satellites, but also smaller rockets that are used to take measuring instruments, also called sounding rockets. These rockets are mostly used to get to around 100 km of altitude, which would be too expensive using bigger rockets, but balloons or other alternatives are not feasible.

In this work, a collaboration was established with CEiiA to develop a sounding rocket, called Morpheus, capable of reaching 100 km of altitude. Besides that, this is an unmanned mission and the sounding rocket is not intended to be reusable. However, some other requirements must be considered. Morpheus should be designed as a single stage rocket and the design should be as modular as possible to allow for a quick assemble and disassemble of different sections of the rocket. Moreover, the design of Morpheus was also selected based on the choice of the propellant and fuel, which were previously chosen and are the Liquid Oxygen (LOx) and Liquid Natural Gas (LNG). Both of these must be kept at cryogenic temperatures in their tanks which is a crucial factor in the selection of not only the design but also the materials.

There are essentially three materials that were used to study each component of the rocket in detail: aluminium, more specifically Al 2219-T851, carbon fiber reinforced polymers (CFRP), and sandwich composite with an aluminium honeycomb core between CFRP skins.

Aluminium is a great choice, especially between metallic materials, due to its high specific strength of 114.8 [MPa/(g/cm^3)] [9], and it is also a reliable material with most of the rockets using it for the past decades. Besides that, aluminium has great properties at cryogenic temperatures. R. P. Reed et al [12] found that at a temperature of 76 K, aluminium exhibits a Young's modulus of 76 GPa, a yield strength of 405 MPa and a ultimate tensile strength of 557 MPa. However, it also has some drawbacks, namely the corrosion effect that happens in contact with carbon fiber, due to galvanic corrosion [13]. That is even more critical if the area of the cathode (CFRP) is very large in comparison to the anode (aluminium). Likewise, CFRP also has good mechanical properties at cryogenic temperatures. Jinxin Meng et al [7] has shown that for 77 K, a quasi-isotropy CFRP has a Young's Modulus of 51.92 $\pm$ 3.0 GPa , and an ultimate strength of 620.83 $\pm$ 51.60 MPa. Besides that, carbon fiber tanks could achieve a weight reduction up to 40% when compared to metallic materials [15, 14]. However, the greater problems with CFRP cryogenic tanks are not the mechanical properties themselves, but rather the incompatibility, especially with liquid oxygen, low-temperature cracking, and the leakage problems. The incompatibility problems of combining LOx with CFRP comes from the strong oxidation of liquid oxygen, associated with cracks of CFRP, which could cause combustion, sparks, and explosions when subjected to external effects, such as collisions, friction, and static electricity [11]. In contrast, when the temperature increases, the mechanical properties of both aluminium 2219-T851 and CFRP become weaker. At room temperature (24℃), the aluminium alloy has an ultimate tensile strength of 455 MPa, whereas at 371℃ it is only 30 MPa [1]. Jie Xu et al [6] tested a high-temperature-resistant (HTR) CFRP and also showed a decrease in both the tensile strength and tensile modulus. However, this result can be explained by the softening of the matrix.

"A sandwich is a three-layered structure consisting of an upper and lower face skin and an intermediate sandwich core", figure 1 [3]. The skin and the core, which in this work is a hexagonal honeycomb, are glued together.

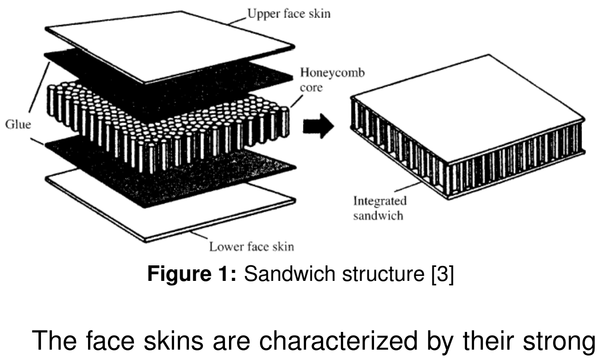

Figure 1: Sandwich structure [3]

The face skins are characterized by their strong resistance in tension and compression, while the core's main role is to ensure a high bending stiffness with a low density material. However, with the increase in the core thickness, it is also expected a contribution to the overall in-plane stiffness. But the effective core stiffness is a nonlinear function of the total core thickness as a result of the core deformations and displacements relative to the skin. The effect of the core thickness is shown in figure 2. As the thickness of the honeycomb core increases, the in-plane properties become more isotropic.

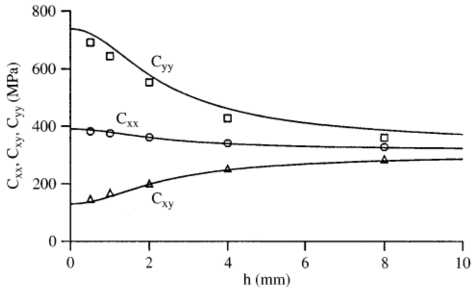

Figure 2: Effect of the core thickness h in the core stiffness C_{xx}, C_{yy}, C_{xy}

In the analysis that will be done during this work, the properties of the honeycomb were kept constant regardless of the thickness of the honeycomb. This does not correspond entirely to the real case as it was demonstrated in this section, so a careful approach should be taken when increasing the thickness of the honeycomb. Besides that, an increase in thickness also increases the manufacture difficulty and the probability of debonding.

After defining the mission requirements and the advantages and disadvantages of some of the most important materials, the development of the objectives of this work was started. There are two main objectives of this work. The first one is to design a sounding rocket with all the requirements that were stated before. Then, the components of this sounding rocket, especially in the aft skirt area of the rocket, were studied in greater detail with a finite element analysis to get the best design possible, i.e. a design that can withstand all the applied loads while keeping the mass as low as possible.

2. Sounding rocket design

The design of Morpheus in this work was a general design. This is only a preliminary design and does not include all the details, but only a first design of each section of the rocket and how they will be assembled.

The main sections of the rocket, the nose cone, and both the propellant and fuel tanks are the starting point of the design of the rocket. The aluminium has been used for many decades in the aerospace industry making it a reliable option, besides that it is easy and cheap to manufacture. On the other hand, a CFRP would allow for a weight reduction but would need to be further studied the impact of cryogenic temperatures as well as possible compatibility issues with the fuel and propellant. In order to reduce the cost, save time, and guarantee a safer option it was chosen that the tanks should be made out of aluminium. Besides that, the nose cone should be made out of carbon composite, which has better mechanical properties than aluminium at high temperatures, and with some thermal protection to obtain the lighter model possible while delivering the aerodynamic performance desired.

The avionics (between the nose cone and the propellant tank), the inter-tank section, and the aft skirt do not need to withstand very high or very low temperature, neither big pressures, so they can be very light since they only need to resist the weight of the rocket and the elevated acceleration of the rocket itself. For these reasons, a CFRP composite laminate should cover the structural components with a possible a reinforcement in some specific areas. However, since the tanks are made out of aluminium and these sections are made of CFRP composite laminates, the connection between them should be with screws. Even though recent studies have shown that it is possible to use friction stir welding to join aluminium to carbon fiber, this is not yet a reliable option [5]. Besides that, the connection with screws allows for a quick assemble and disassemble.

A Y-ring part of aluminium, figure 3, must be welded to the tank which will then be used to connect the tanks to the fuselage. In figure 3, it is also shown the connection between the y-ring and the fuselage, through a female rivet nut and a screw. The y-ring was already used in many aerospace applications, including the Saturn V.

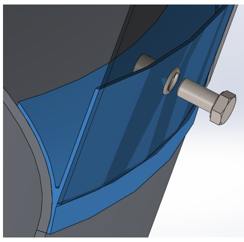

Figure 3: Y-ring (in blue), rivet, and bolt

Inside the fuselage of the avionics sections, a support of carbon fiber will be used to mount all the avionics needed, for that a component with an "L-shape" will be screwed to the fuselage and to this support, figure 4. The same approach will be used to connect the thrust frame to the fuselage in the aft skirt. A door would also be located in the avionics section, inter-tank, and aft skirt, to allow for a quick access and also to have a way to fill the tanks before launch.

In this section, the tube that came from the propellant tank must be connected with screws and nuts to the downcomer that will go through the fuel tank to deliver the liquid oxygen to the motor, figure 5.

The exterior of the tanks will also be the fuselage in that section, allowing for a saving in weight. The tanks should also have anti-vortex and anti-

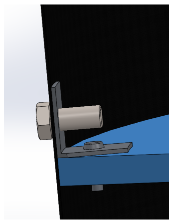

Figure 4: L-shape component

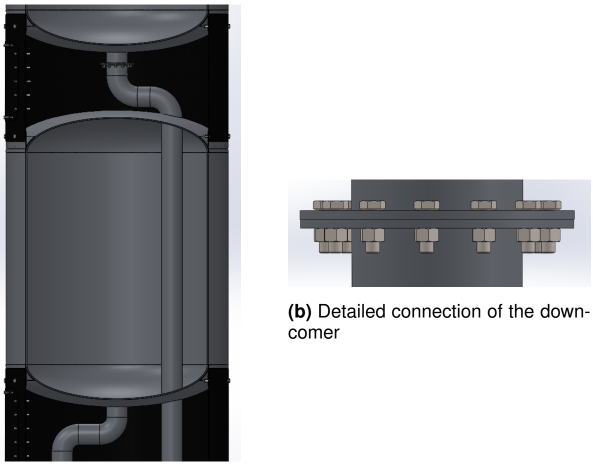

(a) Downcomer going through the fuel tank

(b) Detailed connection of the downcomer

Figure 5: Downcomer

slosh components but these parts were not represented in the final design. In this design, it is not represented any composite overwrapped pressure vessel (COPV), but they should be placed at the top of each tank to keep the pressure constant inside the tanks. Besides that, the electronic cables that go through the sounding rocket should go over the exterior of the rocket through small holes in the fuselage. These small holes should not cause any structural problems since they are not located in critical areas like the tanks. However, a more detailed study should be done in future work.

Another important characteristic that should be taken into consideration when joining different components is the thickness and accessibility of those same components. Since the thickness is too small to have a screw thread, a female rivet nut is first applied and then the screw is screwed to the female rivet, joining the two components in this way (shown in figure 3). This is also helpful because it does not require access to the interior of the rocket to apply neither the rivet nor the screw. This method was designed to join every component of the rocket except for the downcomer, where a screw and a nut are applied to guarantee that there are no leaks of fluid in the downcomer connection (shown in figure 5b). However, if the screws, rivets, and nuts are made out of aluminium, an electrically insulating material or a protective coating must be applied to prevent the oxidation of the aluminium due to the galvanic corrosion caused by the CFRP. Another alternative is to use titanium in these connection components. Similar to aluminium, titanium also has a very high specific strength of 77.3 [MPa/(g/cm^3)] [9], but this value is lower than the aluminium value, which would increase weight.

The only components that are welded are the tanks to the y-ring. For this, the friction stir welding is the preferable choice. This welding technique does not need to reach the material melting point and does not need a filler material which is a great advantage in space application since it does not add more weight. Besides that, the residual stresses and distortions developed are much lower in comparison to other welding methods. Moreover, friction stir welding offers good resistance to corrosion and does not consume the nature of the welding tool. Yet, the equipment needed for this welding requires a high initial cost and needs good support tooling. The final design is shown in figure 6.

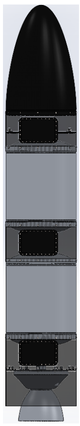

Figure 6: Final design of the sounding rocket

3. High performance materials

The aluminium 2219-T851 was analysed as an isotropic material and its properties, which were previously provided by CEiiA, are shown in Table 1. In addition, it is also necessary to define the ultimate tensile strength of aluminum. Based on the MatWeb data sheet, an aluminum plate with thickness between 6.35 mm and 50.8 mm has an ultimate tensile strength of 425 MPa [10].

Table 1: Aluminium 2219-T851 properties

Modulus of elasticity [GPa]	Shear modulus [GPa]	Poisson's ratio	Density [kg.m^{-3}]	Thermal expansion coefficient [K^{-1}]	Reference temperature for thermal loading [K]
73.1	27.0	0.33	2840	2.41E-05	300

The properties of the carbon fiber were also previously provided by CEiiA and some considerations needed to be taken into account to analyse some components in *NX Siemens* software. For the first analysis of Morpheus' components, it is a good approximation to consider carbon fiber as an orthotropic material. The mechanical properties are available in Table 2, such as Young's Modulus (E), shear modulus (G), and Poisson's ratio (ν, in *NX Siemens* is referred to by the GU symbol). However, the Poisson's ratio was considered the same in all directions since it was only given one value and it is a good approximation for this kind of analysis. The allowable tensile stress (ST), compression stress (SC), and shear stress (SS) are shown in Table 3. The carbon's fiber density is 1210 kg.m^{-3} and the failure criteria used was the Tsai-Wu.

Table 2: CFRP ply: mechanical properties

E_1 [GPa]	E_2 [GPa]	E_3 [GPa]	G_{12} [GPa]	G_{13} [GPa]	G_{23} [GPa]	ν_{12}	ν_{13}	ν_{23}
264	241	241	295	280	280	38.3	20	20

Table 3: CFRP ply: Stress limits

ST_1 [MPa]	ST_2 [MPa]	ST_3 [MPa]	SC_1 [MPa]	SC_2 [MPa]	SC_3 [MPa]	SS_{12} [MPa]	SS_{13} [MPa]	SS_{23} [MPa]
264	241	241	295	280	280	38.3	20	20

The aluminium honeycomb was chosen from HexWeb®. Since some of the properties were not given in the available datasheet such as the Young's modulus in direction 1 and 2 and inplane shear modulus, and because they are required to perform the calculations in the *NX Siemens* software, it was considered a small value (0.01 MPa) for these parameters which is a good approximation considering that the main objective of the honeycomb is to resist shear loads and buckling and it is very weak in those directions when comparing to the modulus in the vertical direction, direction 3. Since the Poisson's ratio in the directions 13 and 12 are not required for the calculations, it was not introduced in the software. As for the stress limits, the available values were introduced to the software and for the others is was considered a negligible value of 0.01 MPa which is a good approximation for this honeycomb. All these values are shown in Table 4 and, also in Table 5.

Table 4: Honeycomb: mechanical properties

E_1 [MPa]	E_2 [MPa]	E_3 [MPa]	G_{12} [MPa]	G_{13} [MPa]	G_{23} [MPa]	ν_{12}	ν_{13}	ν_{23}
0.01	0.01	2826.85	0.01	689.48	220.63	0.49	—	—

Table 5: Honeycomb: Stress limits

ST_1 [MPa]	ST_2 [MPa]	ST_3 [MPa]	SC_1 [MPa]	SC_2 [MPa]	SC_3 [MPa]	SS_{12} [MPa]	SS_{13} [MPa]	SS_{23} [MPa]
0.01	0.01	0.01	0.01	0.01	8.34	0.01	3.57	2.12

One of the advantages of this Flex-Core® honeycomb is that it permits "small radii of curvature without deformation of the cell walls or loss of mechanical properties" [1], as shown in figure 7.

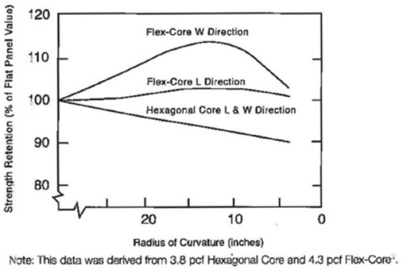

Figure 7: Effect of the radius of curvature in the strength retention [1]

Hexcel also offers a "vented "Flex-core. The vented structures offer thermal protection due to the low thermal conductivity while also preventing the pressure from debonding the sandwich structure, as is shown in figure 8. "The venting is a rectangular shaped vent in the free cell wall of the flexcore honeycomb" [1].

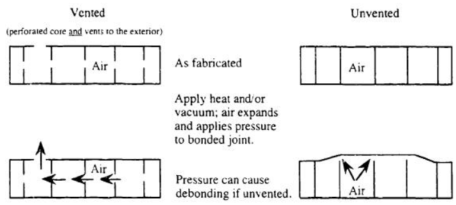

Figure 8: Vented versus unvented honeycomb structures

4. Methodology

All the operational loads were previously provided by CEiiA. Since this is only a preliminary study, it was only considered the main forces, which are the thrust and the rocket's weight at its center of mass. The origin of the reference system is located at the nose cone and the negative axis of the vertical coordinate, which is considered to be the *z* component, points towards the center of the thrust frame. In this case study, the sum of all the components of the rocket is 997.021 kg, and the center of mass of the rocket at z = -3.64 m. These values were obtained based on the initial assumptions of CEiiA. As for the thrust, it was studied the case where the thrust is 25250 N and makes an angle of 8 °with the vertical axis. The thrust is applied in a point that projects over a circle with 0.2 m in diameter.

After specifying the forces that should be applied, a finite element analysis was done with 2D elements with the *NX Siemens* software.

Finally, the connection elements used to simulate the screws, the connection to the mass or the thrust were the "RBE2" and "RBE3". RBE2 elements are considered rigid elements because they do not allow for relative movement between different nodes. On the other hand, RBE3 elements allow for relative movement between different nodes and, this type of element connection distributes the applied force according to the distance between

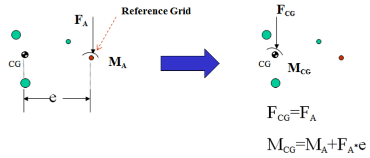

(a) First step

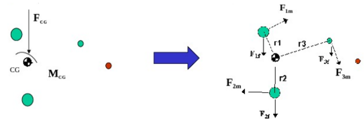

(b) Second step

Figure 9: RBE3 element connection mechanics

the center of gravity and the nodes. As for the moment, this is not applied as a moment to the nodes, instead, forces in different directions are applied to the node derived from the moment at the center of gravity, as it is shown in the schematic example of figure 9.

To design each component according to the materials, two different options of *NX Siemens* were selected. It was used the "laminate" option to simulate the composites with carbon fiber and the honeycomb. As for the aluminium, the "PSHELL" was the selected option. Before optimising the design of each component a few considerations needed to be attended first. Since the optimization of the design was made through experimentation with different thicknesses and angles, and it is not possible to try out every single combination, some conditions were previously defined. Each carbon fiber's ply has a thickness of 0.25 mm and the total thickness of carbon fiber is chosen by adding or removing fiber. Also, the angle of the fiber orientation was chosen to optimize for the structural performance. These angles varied by 15 degrees in each trial. Finally, the core was considered as just one ply and its thickness could vary by 1 mm in each trial. On the other hand, in each iteration, the variation of aluminium thickness was 0.5 mm.

4.1. Thrust frame

The model of the thrust frame has 12 holes with 12 mm in diameter, which would then be used to connect to the fuselage of the aft skirt with the "L-shape" component mentioned in section 2. Also, it was created a circle within the origin of the center of these smaller holes and, with 28 mm of diameter. This circle allowed for a more detailed study of the region near the holes with more elements which resulted in a better representation of the reality. Besides that, it was introduced a circle with 200 mm in diameter in the center of the thrust frame to simulate the thrust area as it was referenced before. There are also two holes in the middle that simulated the tubes of fuel and propellant that would connect to the motor. Since this is a

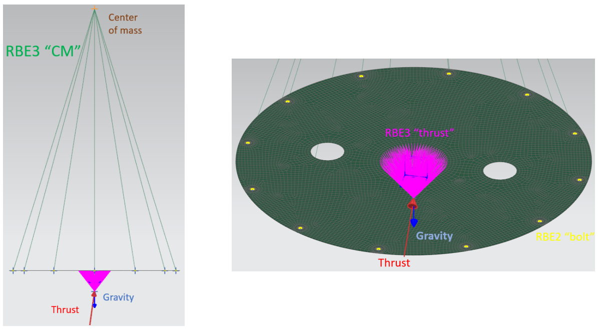

Figure 10: Applied forces and RBE connections

first model, all the other supports that are needed to fix the motor are not represented and there is no reinforcement in any of the holes, but this simpler model is enough for a first iteration to get an approximation of the final results. A mesh with "CQUAD4" elements of 10 mm in size was used, with a mesh control applied to the small holes.

For the thrust frame model, a RBE2 connection was used to design the bolt that is going to be present in the smaller holes, because the bolt is a rigid element that should not allow for any relative movement between different nodes of the hole. However, RBE3 elements are used to connect the holes to the center of mass and from the area at the center of the thrust frame to the point where the thrust is applied, figure 13. This is a more conservative approach that does not transmit any rigidity from the structure of the rocket while also allowing the relative movement of the nodes.

4.2. Aft Skirt frame

The aft skirt was first modeled based on some previous assumptions. There should be 12 holes with 12 mm that would connect to the thrust frame. It is also important to note that the region under these holes is only a fuselage cover and it is not expected to resist any structural loads. In the upper part of the aft skirt, there are also 12 holes that will be used to join the aft skirt to the y-ring of the fuel tank. These holes were also considered to have 12 mm in diameter to minimize the stress concentration. Between the upper region and the area of the thrust frame, there is a door that would allow for quick access to the inner part of the rocket. This door would be screwed to the aft skirt in 28 holes with 8 mm in diameter.

For the aft skirt, there are some important features that were studied which required some special details when considering this surface model. It was considered columns that would reinforce the structure of the aft skirt from the top holes to the bottom holes, except for the holes that are present in the middle of the door. Besides that, it was also created a circular region in the upper part of the

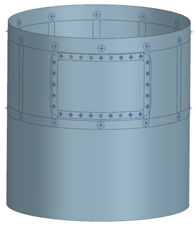

Figure 11: Surface of the aft skirt model

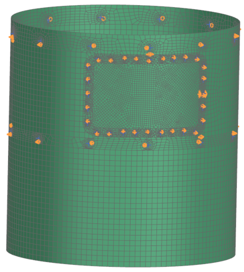

Figure 12: 2D mesh for aft skirt and the mesh controls used in orange

aft skirt to simulate the y-ring which would give a structural reinforcement to the structure. Furthermore, the lower part of the aft skirt was separated from the area of the thrust frame, because this is not a critical area of the rocket regarding the impact of the applied loads. So this lower part does not need as much material as the other areas which could save weight while guaranteeing the desired performance. Finally, surrounding the holes of the aft skirt and the door, it was created a circular region around them to simulate these areas in more detail, using more elements. This model is shown in figure 11. However, this region should have a reinforcement due to the high concentration of stress near that region. For this reason, and to have a good estimation of the reality for the rest of the component, the area surrounding the holes was not considered, that is if this area had a failure index above one the overall component, it was still considered safe.

A mesh with "CQUAD4" elements was used alongside with several mesh control regions, as shown in figure 12.

In this model, only RBE2 elements were used. The RBE2 elements that connect to thrust (13a in yellow) and the RBE2 elements that connect from the upper holes to the center of mass (13a in blue) were chosen to provide some additional rigidity to the model, which RBE3 does not provide. Although this estimates a better than expected scenario, it is closer to the reality than an RBE3, since there cannot be any significant relative movement between these holes, which otherwise could cause a catastrophic failure. Moreover, both the y-ring, which is connected to the fuel tank, and the thrust frame provide the rigidity, which was intended to be simulated by the RBE2 elements, when they are con-

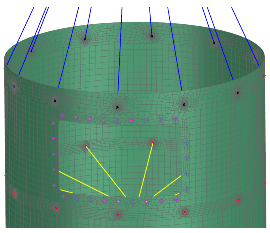

(a) RBE2 connections in the aft skirt

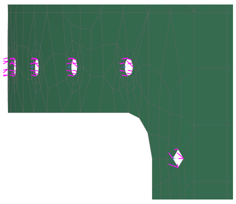

(b) Detailed RBE2 connection from the aft skirt to the door

Figure 13: Element connections in the aft skirt

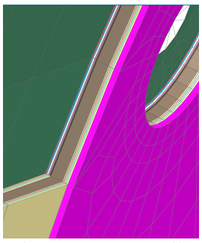

Figure 14: Example of the laminate offset, with an aluminium part in pink, and the layers of the composite aligned

nected to the aft skirt. RBE2 elements were also used in the holes of the upper region (13a in black) and the thrust frame's region (13a in red). These elements simulate the bolts and screw connection. Finally, for the remaining connection of the door to the aft skirt, RBE2 elements were also used, as it is shown in pink in figure 13b. This connection guarantees that each hole of the aft skirt is connected to the holes of the door while allowing the relative movement between different holes.

Besides that, it must be guaranteed that all the different sections are aligned in the exterior part of the aft skirt, and not in the middle or bottom as it could be the case due to different thicknesses sizes, figure 14.

5. Results & discussion

5.1. Thrust frame

The thrust frame was studied based on a static analysis with the solution type of "SOL 101 Linear Statics - Global Constraints" of *NX Siemens* with the "inertia relief" option activated. This option allows the simulation of an unconstrained structure in a static analysis. A factor of safety of 1.44 was considered, which was obtained by multiplying the average values of the project factor (1.15), model factor (1.05), and yield factor (1.175) which are indicated in the European Space Agency documentation [4].

It was studied the design with a sandwich material, with CFRP and aluminium honeycomb, an aluminium thrust frame, and finally a thrust frame with only carbon fibers.

For the sandwich design the following method was initially considered:

1. Start with a 20 mm core
2. Obtain the minimum number of carbon fiber plies, with a sequence of [0°,+45°], until the failure
3. Reduce the thickness of the core until failure
4. Calculate the final weight
5. Increase the initial thickness of the core by 10 mm and repeat the process from point 2 through 5

The results are shown in Table 6.

Table 6: First optimization for a composite thrust frame

Core [mm]	CFRP skin (one side) [mm]	Mass [kg]
20	3.75	9.88
29	1.5	6.24
34	1.25	6.27

However, it was still possible that the minimum weight possible could be obtained for a higher number of carbon fiber flies, and subsequently a lower core thickness, these results are shown in Table 7.

Table 7: Final optimization for a composite thrust frame

Core [mm]	CFRP skin (one side) [mm]	Mass [kg]
29	1.5	6.24
24	1.75	6.21
22	2	6.5

In conclusion, a thrust frame with a core of 24 mm and 7 plies of carbon fiber with 0.25 mm thickness provides the lightest thrust frame possible that can withstand the forces which it will be subjected to, figure 15.

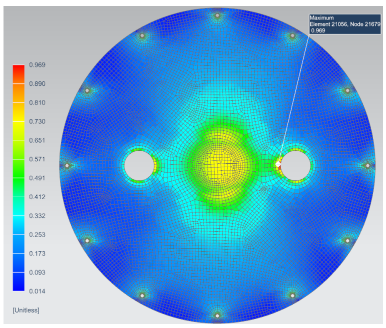

Figure 15: Maximum failure index (elemental-nodal) for the final thrust frame with 24 mm of an aluminium honeycomb's core and 7 plies of 0.25 mm carbon fiber on each side

On the other hand, the aluminium design requires a thickness of 10 mm, corresponding to 24.11 kg of mass, while the thrust frame made out of only carbon fibers needs 63 plies with a total weight of 16.18kg. To sum up, the sandwich design is the preferable choice.

5.2. Aft skirt - static analysis

The objective of this section is to arrive at the best possible design not only for the aft skirt but also for the door. For this component of the rocket, it is not only important a static analysis but also a buckling analysis. It is possible to consider the structure of the aft skirt as a cylindrical column that is being compressed on both ends. In the case of the aft skirt, the compression occurs in the top part due to the mass of the rocket that is above it, and from the bottom part because of the thrust that is being applied. These forces can cause a loss of stability that leads to a buckling failure. The simulations for the static analysis did not consider a factor of safety during the analysis, but it was considered in the final design, which has the factor of safety required.

First of all, it should be noted that the model of the aft skirt has a lot of different combinations possible and, because of that a sequential analysis process needs to be considered. In the first simulations, it was clear that the lower part of the skirt was not a concern regarding the possibility of a failure caused by the applied forces. Accordingly, the lower part of the skirt was tested with only 3 plies of carbon fiber and, yet, this region was still not the point of failure. It was possible to reduce even more the number of plies which would, correspondingly, reduce the weight. However, if the number of plies is reduced even more, other problems start to emerge, such as the thermal conditions that could start to melt the carbon fibers. Nevertheless, a more detailed study should be done in future works.

In this model, two different components are being considered, the aft skirt itself and the door. By analysing these two components simultaneously the point of failure was many times present in the door, which did not allow for the optimization of the aft skirt itself. Therefore, the door was removed from the simulation and, instead, multiple RBE2 from the edge of the opening of the door were connected to the center of this area as it is shown in figure 16. In this way, it was guaranteed that there was no relative movement between different points in the edge. This increased the rigidity of this region more than the door could because the RBE2 elements have an infinity rigidity, but this is a good approximation and, after optimizing the aft skirt, the door is going to be again introduced to make sure that the approach taken by using the RBE2 was a good consideration and that the complete structure can resist all the applied forces. Besides that, as for the CFRP orientation, the plies were simulated based on a sequence of [0°/45°] as it is shown in figure 17.

Firstly, the impact of the aluminium columns was studied, however, the conclusion indicated that it is better to add one more carbon fiber to the aft skirt fuselage than to add 1 mm of aluminium columns. For this reason, these columns were removed from the design. Following this, the y-ring was tested. Figure 18 shows that the model with 2 mm of CFRP and 1 mm of an aluminium y-ring is the best design possible.

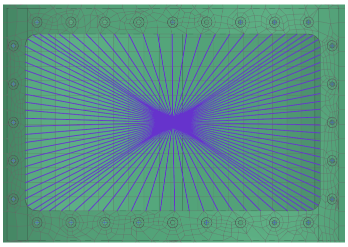

Figure 16: RBE2 elements replacing the door

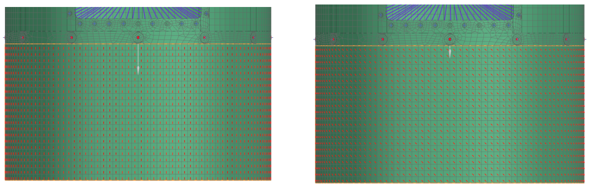

(a) 0°fibers **(b)** 45°fibers

Figure 17: Aft Skirt fiber orientation

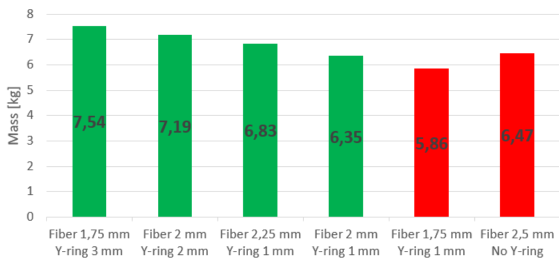

Figure 18: Weight of the aft skirt when testing for the aluminium y-ring. The color red indicates the failure of the structure, while the green color corresponds to a safe model

After this, the honeycomb aluminium's core was tested. It was added to the aft skirt, except to the lower part of this component. The core was aligned normal to the circular face. The results are shown in figure 19.

Although the honeycomb in the middle of the fuselage of the aft skirt could save some weight, this is a small difference that does not justify the difficulty in the manufacture. Additionally, it would also increase the cost not only in the manufacture, but also in the material itself since these small honeycomb thicknesses are not standard dimensions and they would need to be obtained through a special request with possible implications in the properties of the material itself. Grünewald et al. [8] described that 3D sandwich structure like a circular shape can be manufactured, however the more complex the curvature, the greater the challenges in the manufacturing process. Also, the manufac-

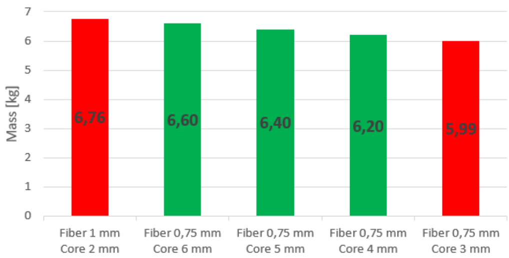

Figure 19: Weight of the aft skirt with a honeycomb core. The color red indicates the failure of the structure, while the green color corresponds to a safe model

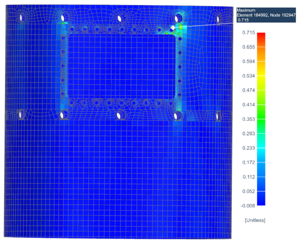

(a) Final model of the aft skirt

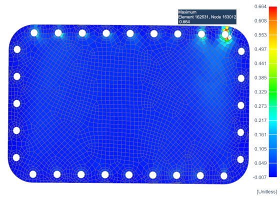

(b) Final model of the door

Figure 20: Failure index

turing imperfections of the core or the interfaces between the skins and the core for cylindrical panels usually fail due to buckling [2]. Besides that, in this case, the honeycomb core is only being applied at the upper region of the aft skirt which would be difficult for the manufacturing process if the aft skirt would be manufactured as one piece. All these increase difficulties which would also increase the economic cost does not justify the small difference in weight of 0.15kg which corresponds to only 2.4% of the total weight of the aft skirt. Due to these reasons, the study of the aft skirt was continued with 8 CFRP plies in the upper region of the aft skirt.

After this, the RBE2 elements that were used to simulate the door were replaced for the door itself, and the door was connected to the aft skirt through RBE2 elements as was explained in 4.2.

Firstly, a door made out of only carbon fiber plies was tested. The first design consisted of an 1 mm thickness door, but this model failed not in the door itself but in the aft skirt. Even though the amount of carbon fiber plies was increased and decreased, a failure remained to be present in the aft skirt. So, the aft skirt thickness was increased to 2.25 mm which corresponds to nine carbon fiber plies. In this model, a door with 0.75 mm was proven to be the lightest model possible with the failure index below 1.

This final design with an aft skirt of 2.25 mm and a door with 0.75 mm with a mass of 6.83 kg and 0.21 kg respectively, which gives a total weight of 7.04 kg for the model. Although a factor of safety was not considered during this analysis, this model has almost the factor of safety required, since the maximum failure index corresponds to 0.715, which multiplied by the factor of safety of 1.44 results in 1.0296. The failure index of this model is shown in figure 20.

A door with a honeycomb core in the middle, and an aluminium door were tested. However, both of these designs required a heavier door to withstand the operational loads.

An aluminium aft skirt was also tested, but the lightest model possible had 10.79 kg of mass, corresponding to an aft skirt with 10.47kg and an aluminium door with 0.32kg.

5.3. Aft skirt - buckling analysis

The buckling analysis was done with the "SOL 105 Linear Buckling" solution of *NX Siemens*. In this solution, a buckling mode below 1 means that the structure is unstable and will fail due to buckling.

The final model that was obtained in the static analysis, failed with a buckling mode of 0.977. So, the number of CFRP plies of the door was increased to 4, resulting in a first buckling mode of 1.18. However, this does not guarantee the factor of safety required of 1.44. To have a model with the required factor of safety, a door with 2 mm of CFRP is necessary, and the respective results are shown in figure 21.

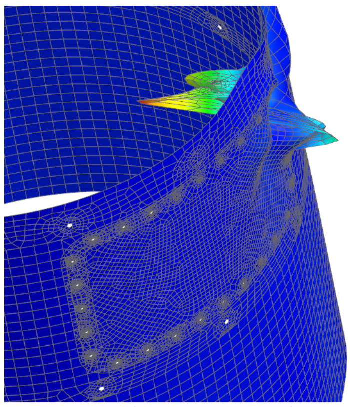

Figure 21: First mode of buckling (1.59) for the final design

To sum up, the final design of the aft skirt and the door consisted in: 1 mm aluminium Y-ring, a lower fuselage with 0.75 mm of carbon fiber, and the rest of the fuselage with 2.25 mm of CFRP, corresponding to a weight of 6.83 kg. Additionally, the final model of the door corresponded to 8 carbon fiber plies, giving a total of 2 mm thickness and 0.55 kg of mass.

6. Conclusions

From the literature review, it was evident that composite materials are becoming an essential material in aerospace applications replacing metallic materials. Although composites allow for a reduction of weight when compared to metals, they also have some drawbacks, such as the incompatibility with liquid oxygen. Nevertheless, in the conceptual design the carbon fiber was used in most of the components, except for the tanks, y-ring, and downcomer. On the other hand, there are big concerns regarding the oxidation of aluminium parts when in contact with carbon fiber. For this reason, the bolts used should be made out of titanium to solve this problem, even though this is a heavier material.

Secondly, a first design of the thrust frame, the aft skirt, and its door were obtained. This first iteration did not consider any reinforcement, specially in critical areas such as the holes, or thermal protection. The lightest design for the thrust frame consisted of a core with 24 mm and 7 CFRP plies with 0.25 mm on each side. This amounts to a total weight of 6.21 kg. On the other hand, for the aft skirt, a similar approach in the static analysis was done but an additional buckling analysis was simulated. In the final design, the region below the thrust frame consisted of only three CFRP, while the rest of the aft skirt was made out of 2.25 mm in carbon fiber, with an additional 1 mm of aluminium at the top representing the Y-ring. This model weighs 6.83 kg. The door required 2 mm of carbon fiber to resist all the applied loads, making a total of 0.55 kg. Even though many simplifications were done, a factor of safety was considered, representing a less than ideal situation, thus constituting a good starting point for further iterations.

7. Acknowledgments

This work could not be possible without the collaboration of Dr. André Guerra from CEiiA and professor Aurélio Araújo from Instituto Superior Técnico.

References

[1] Hexweb® aluminum flex-core® formable aluminum honeycomb, 2017. Accessed on 07-09-2021.

[2] P. R. A. Muc, A. Stawiarski. Experimental investigations of compressed sandwich composite/honeycomb cylindrical shells. *Applied Composite Materials, An International Journal for the Science and Application of Composite Materials*, 25:177 – 189, June 2017.

[3] W. Becker. *Archive of Applied Mechanics*, volume 68, chapter The in-plane stiffnesses of a honeycomb core including the thickness effect, pages 334–341. pringer-Verlag 1998, 1998.

[4] E. C. for Space Standardization ECSS. Space engineering – mechanical – part 2: Structural. Technical Report ECSS-E-30 Part 2A, ESA - European Space Agency, April 2000.

[5] S. L. H S Bang, Atanu Das. Friction stir lap joining of automotive aluminium alloy and carbon-fiber-reinforced plastic. In *IOP Conf. Ser.: Mater. Sci. Eng. 369 012033*, 2018.

[6] Q. H. Jie Xu, Weixin Wang. Mechanical properties of pultruded high-temperature-resistant carbon-fiber-reinforced polymer tendons at elevated temperatures. *Elsevier - Construction and Building Materials*, 258(119526), 2020.

[7] H. Y. Jinxin Meng, Yong Wang. Mechanical properties and internal microdefects evolution of carbon fiber reinforced polymer composites: Cryogenic temperature and thermocycling effects. *Elsevier*, (108083), February 2020.

[8] P. P. Jonas Grünewald and V. Altstädt. Manufacturing of thermoplastic composite sandwich structures: A review of literature. *Journal of Thermoplastic Composite Materials*, 30(4):437–464, 2017.

[9] K. Kowalczyk-Gajewska. *Micromeachanical Modelling of metals and alloys of high specific strength*. Instytut Podstawowych Problemów Techniki Polskiej Akademii nauk, 2011.

[10] MatWeb. Aluminum 2219-t851. Accessed on 19-09-2021.

[11] F. L. Ni Liu, Bin Ma. Progress in research on composite cryogenic propellant tank for large aerospace vehicles. *Elsevier - Composites Part A*, 143(106297), 2021.

[12] N. S. R.P. Reed, P.T. Purtscher. *Aluminum alloys for Als cryogenic tanks: comparative measurements of cryogenic mechanical properties of Al-Li alloys and Alloy 2219*. Phillips laboratory - Propulsion Directorate - Air force systems command, Edwards Air Force base CA 93523-5000, February 1993.

[13] C. Staff. An introduction to the galvanic series: Galvanic compatibility and corrosion, 2020. Accessed on 19-10-2021.

[14] K. O. Yonemoto koichi, Yamamoto Yuta. Application of cfrp with high hydrogen gas barrier characteristics to fuel tanks of space transportation system. *Trans Japan Soc Aeronautical Space Space Technol Japan*, 7(26):8–13, 2019.

[15] G. C. Zhan L.H. Analysis of research status of composite cryotank for space. *Aeronautical Manufacture Technolgy*, 62(16):79–87, 2019.